

MOSQUITO HEARING: SOUND-INDUCED ANTENNAL VIBRATIONS IN MALE AND FEMALE *Aedes aegypti*

MARTIN C. GÖPFERT*, HANS BRIEGEL AND DANIEL ROBERT

Institute for Zoology, Laboratory of Bioacoustics, University of Zürich, Winterthurerstrasse 190, CH-8057 Zürich, Switzerland

*e-mail: mgoepfer@zool.unizh.ch

Accepted 26 July; published on WWW 30 September 1999

Summary

Male mosquitoes are attracted by the flight sounds of conspecific females. In males only, the antennal flagellum bears a large number of long hairs and is therefore said to be plumose. As early as 1855, it was proposed that this remarkable antennal anatomy served as a sound-receiving structure. In the present study, the sound-induced vibrations of the antennal flagellum in male and female *Aedes aegypti* were compared, and the functional significance of the flagellar hairs for audition was examined. In both males and females, the antennae are resonantly tuned mechanical systems that move as simple forced damped harmonic oscillators when acoustically stimulated. The best frequency of the female antenna is around 230 Hz; that of the male is around 380 Hz, which corresponds approximately to the fundamental frequency of female

flight sounds. The antennal hairs of males are resonantly tuned to frequencies between approximately 2600 and 3100 Hz and are therefore stiffly coupled to, and move together with, the flagellar shaft when stimulated at biologically relevant frequencies around 380 Hz. Because of this stiff coupling, forces acting on the hairs can be transmitted to the shaft and thus to the auditory sensory organ at the base of the flagellum, a process that is proposed to improve acoustic sensitivity. Indeed, the mechanical sensitivity of the male antenna not only exceeds the sensitivity of the female antenna but also those of all other arthropod movement receivers studied so far.

Key words: antenna, vibration, auditory biomechanics, bioacoustics, sound perception, Johnston's organ, mosquito, *Aedes aegypti*.

Introduction

Insect hearing organs can be divided in two distinct classes: tympanal ears, which are sensitive to the pressure component of sound, and movement receivers, which respond to oscillations of air particles in the sound field (for reviews, see Bennet-Clark, 1971; Michelsen and Nocke, 1974; Tautz, 1979; Hoy and Robert, 1996). Movement receivers are usually light structures such as sensory hairs or antennae that are deflected by the sound-induced oscillations of air particles. One of the classic examples of an insect movement receiver is the plumose antenna of male mosquitoes.

The presence of an acoustic sense in mosquitoes was first reported by Johnston (1855) when he discovered a sensory organ in the second segment of the mosquito antenna, subsequently named Johnston's organ. Johnston's functional predictions were later confirmed by multiple behavioural observations (e.g. Roth, 1948; Tischner and Schieff, 1955; Wishart and Riordan, 1959): flying mosquitoes produce sounds with their wing stroke, and male and female mosquitoes differ with respect to the frequency composition of these sounds. In many mosquito species, both the female's sound emissions and artificial sounds at the genuine frequency elicit positive phonotaxis and precopulatory behaviour in the males. Ablation

experiments (Roth, 1948) indicated that sound induces vibrations of the antennal flagellum that are transmitted to and sensed by Johnston's organ. This was confirmed by stroboscopic observations of sound-induced antennal vibrations (Tischner and Schieff, 1955; Wishart et al., 1962) and by recordings of microphonic potentials from Johnston's organ (e.g. Tischner and Schieff, 1955). Both types of evidence indicated that the antennal flagellum of male mosquitoes is resonantly tuned to the flight sounds of conspecific females (for reviews, see Clements, 1963; Belton, 1974).

The antennae of male mosquitoes demonstrate obvious structural modifications that are absent from the antennae of females. In addition to differences in the structure of Johnston's organ proper, the flagellum of the male antenna is plumose, bearing whorls of extremely long and thin flagellar sensory hairs (also called fibrils). Since the length of these hairs decreases continuously towards the antennal tip, the shape of the male mosquito antenna is reminiscent of a Christmas tree. It has been proposed that antennal hairs are a prerequisite for acoustic sensitivity since, in the males of some mosquito species, for which acoustic communication could not be demonstrated, such antennal anatomy is absent (Clements,

1963). In addition, diurnal changes in the hair position with respect to the main antennal shaft of some mosquito species were suggested to affect acoustic sensitivity (Roth, 1948; Nijhout and Sheffield, 1979). Remarkably, as early as 1874, Mayer reported that single hairs have different best frequencies and respond maximally to the pitch of different tuning forks. He concluded that the hair vibrations are transmitted to the flagellar shaft and enable the males to respond to a wider frequency band, which he thought was advantageous in detecting the range of frequencies of female flight sounds. In more recent reviews, the main function of the hairs was suggested instead to be to increase the antennal surface and therefore to enhance acoustic sensitivity (Clements, 1963; Tautz, 1979). However, the exact function of the antennal hairs in the reception of particle movements remains unknown.

While the study of sound-induced vibrations of sensory hairs in diverse arthropods has made much progress within the last few decades (Tautz, 1977, 1979; Fletcher, 1978; Kämper and Kleindienst, 1990; Humphrey et al., 1993; Kumagai et al., 1998; Shimozawa et al., 1998), much of our present knowledge about the physiology of hearing in mosquitoes is based on reports dating from the first half of this century. The need for a more detailed biomechanical analysis of the mosquito antenna has been pointed out (Michelsen and Nocke, 1974), but such studies have hitherto been precluded by technical limitations arising from the morphological complexity and the small size of the antennae. Recent progress in laser vibrometry technology makes such biomechanical analyses possible. By combining microscanning laser vibrometry with acoustic near-field measuring techniques, we have investigated the magnitude and phase of the velocity response, the deflection shapes and the intensity characteristics of sound-induced antennal vibrations in *Aedes aegypti*. To identify correlations between antennal structure and vibration properties, all measurements were made comparatively in males and females. In addition to the vibrations of the antennal flagellum, the mechanical response of the flagellar hairs was measured to evaluate their role in the process of audition. The results are related to previous studies, and the functional significance of the plumose antennal structure in male mosquitoes is discussed.

Materials and methods

Animals

The culicid species *Aedes aegypti* L. (UGAL strain from Georgia, USA) was raised in the laboratory. Details of rearing conditions are given by Timmermann and Briegel (1993). All experiments were carried out with imagines 3–4 days after eclosion at constant room temperature (22–23°C) to reduce age- and temperature-dependent variations that have been reported to influence both the frequency composition of the flight sounds and the antennal mechanical response (Tischner and Schieff, 1955).

Experimental arrangement

The animals were briefly cooled prior to removal of the wings

and legs and were mounted to a holder using modelling clay. The heads of the animals protruded over the clay and the holder to ensure that the measurements were not influenced by the boundary layer around the holder. The preparation was positioned between the laser vibrometer and the loudspeaker (Fig. 1), all of which were aligned on a vibration isolation table (TMC, type 78-442-12). This linear arrangement was chosen because of the vector properties of the particle velocity component of sound, and it allowed laser measurements to be made coaxially with the direction of antennal movements. The online and coaxial video monitoring system of the laser vibrometer was used to position the laser beam accurately at different locations on the antennal structures (Robert and Lewin, 1998).

Acoustic stimulation and sound field calibration

Sound-induced antennal vibrations were studied in the frequency range between 100 and 3100 Hz. For acoustic stimulation, either continuous band-limited random noise (bandwidth 100–3100 Hz) or pure tones were generated by a Stanford Research Systems network analyser (type SR780). The output signal was amplified (dB-Technologies power amplifier, model PL 500) and fed to a loudspeaker (Uher, type UL 1302) positioned at a distance $r=0.07$ m from the preparation (Fig. 1). Thus, the preparation was located in the acoustic near-field ($r \leq \lambda$, where λ is wavelength) for the stimulus frequencies applied here ($0.11 \text{ m} < \lambda < 3.43 \text{ m}$). Acoustic near-field stimulation is problematic since the magnitude and phase of the particle velocity change rapidly as the distance r decreases relative to the wavelength. In contrast to acoustic far-field conditions, the particle velocity is not proportional, either in magnitude or in phase, to sound pressure. Because of the small distance between

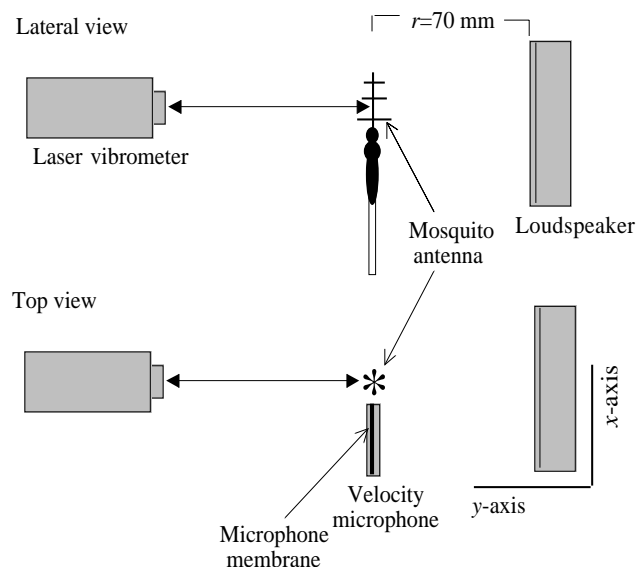


Fig. 1. Experimental arrangement shown in lateral and top views. The laser vibrometer, the mosquito and the loudspeaker were aligned along the optical axis of the laser vibrometer (y-axis; see top view). The particle velocity microphone and the mosquito antenna were positioned at the same distance from the loudspeaker (70 mm).

the loudspeaker and the preparation, it was therefore necessary to measure the particle velocity directly. For this purpose, a miniature velocity microphone (Knowles, type NR 3158, dimensions 5.6 mm×4.0 mm×2.2 mm) was connected to an integrating amplifier (modified from Bennet-Clark, 1984), the output of which was flat (to within approximately ± 0.5 dB) at frequencies between 100 and 3100 Hz (NR 3158 microphone specifications by Knowles Electronics Inc., Itasca, Illinois, USA). Additional far-field ($r=2.5$ m, corresponding to approximately 1.5λ at 200 Hz) calibrations against a precision pressure microphone (Bruel & Kjaer, type 4138) confirmed the amplified output of the velocity microphone to be flat within ± 0.9 dB and to be in phase with the output of the pressure microphone within $\pm 6^\circ$ in the frequency range between 200 and 3100 Hz. The output voltage of the particle velocity microphone increases linearly with increasing particle velocity, as revealed by far-field calibration with 1000 Hz pure tones ($r=69$ cm, which is approximately 2λ at 1000 Hz; Fig. 2). Also, the ratio of the output voltage signal of the velocity microphone to the particle velocity was plotted against the particle velocity to test for the presence of possible slight non-linearities in the microphone response. A linear fit to this plot revealed a slope close to zero (slope 0.06, $r^2=0.01$, $P>0.1$), confirming the absence of even slight non-linearities; as shown below, this is not the case for the vibration response of mosquito antennae.

During the measurements of antennal vibrations, the velocity microphone was positioned close to the side of the measured antenna, with the membrane of the microphone being perpendicular to the direction of sound propagation (Fig. 1). The sound field produced by the loudspeaker was examined in an area 0.02 m×0.012 m around the preparation, with the holder in position (Fig. 3), to evaluate differences between the particle velocity at the position and at the microphone. Pure-tone analysis revealed the overall magnitude of the particle velocity to be flat within ± 1 dB at 200 and 1500 Hz and within ± 2.5 dB at 3000 Hz. The phase characteristics are also almost flat for low frequencies; however, as the frequency increases, significant phase shifts occur along the axis of measurement (y-axis, Fig. 1). Thus, the accuracy of the phase measurements decreases with frequency. However, this effect could be reduced by precisely adjusting the relative y positions of the microphone and the preparation (Fig. 1, see also Fig. 3).

Microscanning laser vibrometry

A Polytec PSV 200 scanning laser vibrometer consisting of an OFV-055 scanning head was used to monitor the mechanical response of the antenna to sound. The position of the laser spot was controlled by an OFV-3001-S vibrometer beam controller and was monitored *via* the coaxial video system of the scanning head. The PSV 200 laser vibrometer allows extremely precise computer-controlled positioning of the laser spot (focused spot diameter approximately 7 μ m) with a resolution of approximately 1 μ m and fast, computer-controlled scanning of predefined measuring points (Robert and Lewin, 1998). The reflection properties of the antennae were sufficient to obtain highly coherent measurements (see Fig. 4), thus obviating the

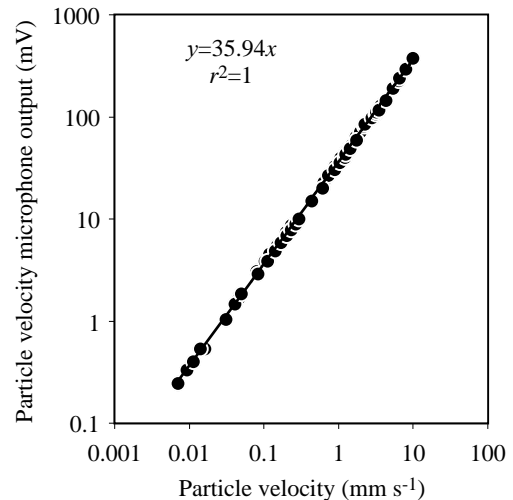


Fig. 2. Intensity characteristics of the velocity microphone revealed by far-field calibration against a Bruel & Kjaer 4138 pressure microphone with 1000 Hz pure tones.

use of reflecting spheres to improve the reflection properties of the antennae.

Flight sound recordings

To compare the frequency characteristics of the antennal vibrations and the flight sound frequencies, we recorded the sounds emitted by tethered flying animals. The mosquitoes were glued dorsally by the pronotum to an insect pin and suspended 10 mm in front of the velocity microphone with the head of the animal pointing towards the microphone. The frequency spectra of the microphone output were calculated by Fast Fourier Transform (FFT) with a frequency resolution of 3.2 Hz. On the basis of the microphone calibrations shown in Fig. 2, the frequency spectra of the voltage output of the microphone were converted to the corresponding particle velocity spectra.

Data acquisition and analysis

The quantities that were actually measured to examine sound-induced antennal vibrations were the magnitude and phase of the particle velocity v_{air} in the sound field (velocity microphone signal) and the magnitude and phase of the velocity response of the antenna v_{vib} (laser signal). The microphone and laser signals were digitised using an Analogic Fast-16 A/D board. A transient window was applied to the data in the time domain prior to analysis. Since the laser measurements had to be taken within a short time to prevent changes in the antennal response caused by desiccation of the animals, only 4–6 subsequent measurements were averaged, which is sufficient to provide a satisfactory signal-to-noise ratio (as estimated using the magnitude squared coherence function; Kates, 1992). The frequency spectra of the magnitude and phase were also estimated using a frequency resolution of 3.2 Hz. The magnitude and phase responses of the antennal vibration velocity were then normalised to the magnitude and phase responses of the velocity microphone by computing transfer functions between the laser and the

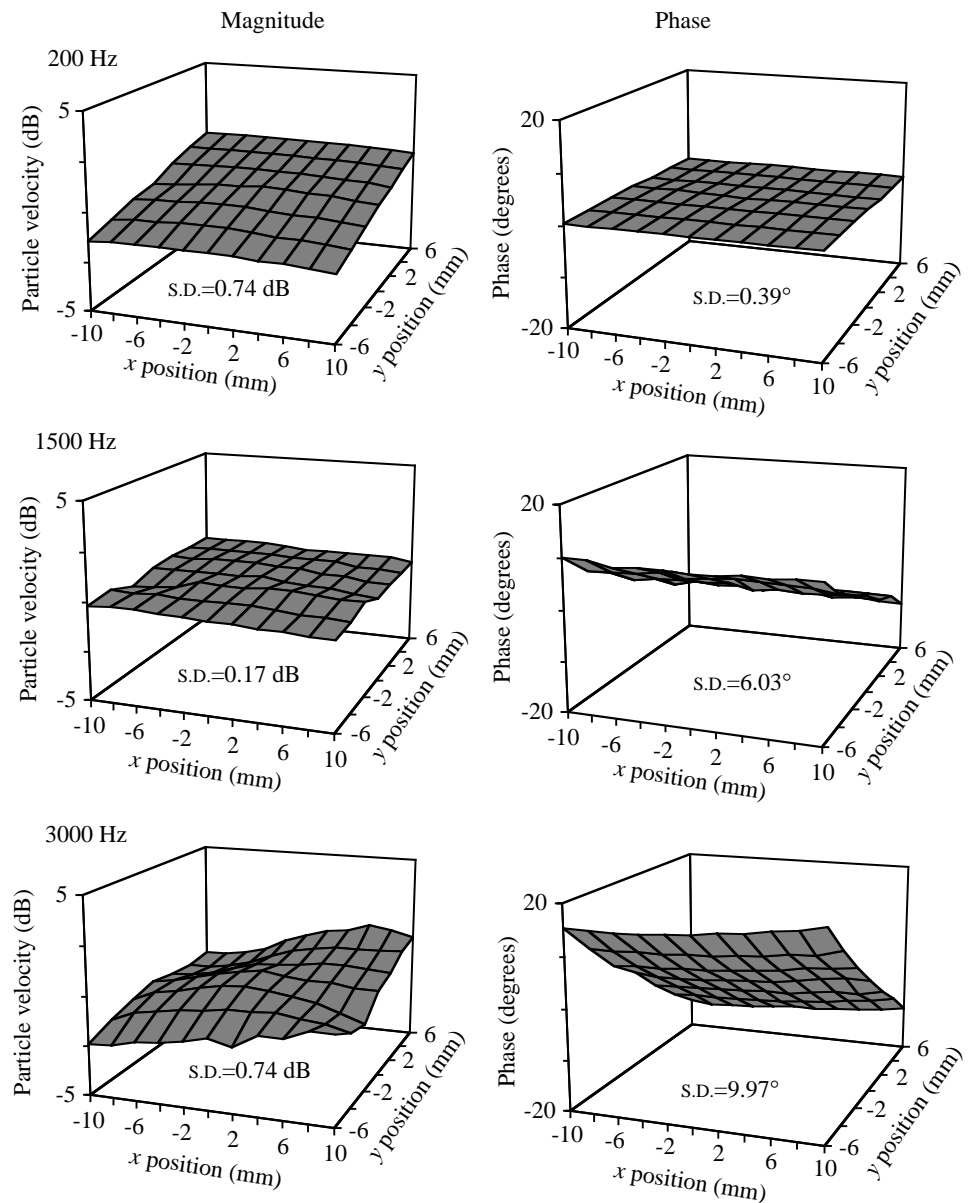


Fig. 3. Magnitude and phase characteristics of the particle velocity of the sound field measured in an area 20 mm×12 mm around the preparation (x - and y -axis convention as in Fig. 1). The y position of the speaker was +70 mm. During experiments, the preparation was positioned at the centre ($x=0$ mm, $y=0$ mm), and the microphone was positioned at $x=+5$ to $+9$ mm and $y=-1$ to $+1$ mm.

microphone signal. The transfer functions were calculated as the cross-powerspectrum of the laser and the microphone signal divided by the auto-powerspectrum of the microphone signal. The noise level in each measurement was examined by computing the coherence function, and only highly coherent measurements (providing phase and amplitude information with minimal contamination from unrelated noise) were used for analysis (Fig. 4). All vibration velocities refer to peak-to-peak velocities, and all values are expressed as means \pm standard deviation (S.D.). Unless otherwise stated, two-tailed Mann–Whitney U -tests were used for statistical analyses.

Results

General structure and vibration response of the antennal flagellum

The structure of the antennae of male and female *Aedes*

aegypti is shown in Fig. 5. In addition to sex-specific differences in the number and length of the antennal hairs, males and females also differ with respect to the length of the antennal flagellum, which is 2 ± 0.1 mm in females and 1.6 ± 0.1 mm in males ($P<0.001$; $N=30$ per sex).

The general frequency characteristics of male and female antennal vibrations were examined in five males and six females by analysing the vibrations of the tip of the antennal flagellum in response to stimulation with band-limited random noise. Frequency spectra of the vibrations of the flagellar tip reveal that the antennae of males and females are resonantly tuned mechanical systems (Fig. 6A,B). The magnitude of the relative vibration velocity, computed as the ratio between the antennal velocity and the particle velocity $v_{\text{vib}}/v_{\text{air}}$, shows a single resonant peak in the frequency range between 100 and 3100 Hz in all the animals studied (Fig. 6A). This peak is accompanied by a shift between the phase of the antennal

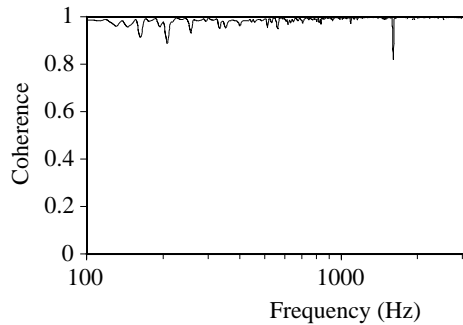


Fig. 4. Characteristic example of the coherence function between the laser and microphone signals during the measurement of sound-induced antennal vibrations. The values of coherence range from 0 to 1. A coherence of 1 indicates that the measurement is not contaminated by external noise.

velocity and the particle velocity of approximately 180° at frequencies around the best frequency (Fig. 6B). Such phase shifts are consistent with the presence of resonance in the mechanical response.

Although the velocity responses of the flagellar tips of male and female *Aedes aegypti* are similar, the best frequencies differ between the sexes (Fig. 6A). The male antennae show best frequencies between 344 and 406 Hz (383 ± 28 Hz), whereas the best frequencies of the female antennae are significantly lower, ranging from 219 to 263 Hz (229 ± 17 Hz; $P < 0.01$). To determine the slopes of the relative vibration velocity at frequencies below and above the best frequency, the magnitudes of the relative vibration velocities (Fig. 6A) were converted to decibels, and logarithmic curves were fitted to the plots. These calculations reveal an increase in the vibration velocity of approximately $+12$ dB per octave at frequencies below best frequency and a decrease in the vibration velocity of approximately -6 dB per octave at frequencies above best frequency for both sexes. The slope below the best frequency

was $+13.2 \pm 0.6$ dB per octave in males (frequency range 100–300 Hz) and $+13.2 \pm 0.4$ dB per octave in females (frequency range 100–200 Hz), and the slope above the best frequency was -7.3 ± 0.9 dB in males (frequency range 450–650 Hz) and -5.8 ± 0.4 dB per octave in females (frequency range 350–600 Hz). At low frequencies, the antennal vibration velocity v_{vib} leads the particle velocity in the ambient air v_{air} by approximately 90° (by $100 \pm 6^\circ$ in males and by $82 \pm 7^\circ$ in females at frequencies between 100 and 125 Hz; Fig. 6B). The phase difference between the antennal velocity and the particle velocity decreases as frequency increases and approaches 0° for frequencies around the best frequency (the mean phase lead at best frequency is $+23 \pm 9^\circ$ for male and $+7 \pm 5^\circ$ for female antennae). A phase lag of -90° is reached at approximately 1000 Hz in females and at approximately 1700 Hz in males, and the phase shift continues towards higher frequencies, indicating the presence of additional resonances at higher frequencies. The Q-values (Bennet-Clark, 1999) of antennal tuning were determined by fitting logarithmic curves to the decibel-converted frequency spectra of the relative vibration velocity magnitudes. The $Q_{3\text{dB}}$ -values of the velocity response of the female and the male are similar, ranging between 1.9 and 3.0 (2.4 ± 0.4 for males and 2.1 ± 0.1 for females; $P > 0.05$).

The antennal vibrations of male and female *Aedes aegypti* also differ with respect to their maximum vibration velocities (Fig. 6A). In both sexes, the velocity of the antennal tip v_{vib} exceeds the particle velocity in the ambient air v_{air} at frequencies around the best frequency (Fig. 6A). The maximum velocity of male antennae is significantly greater than that of female antennae: in males, the maximum antennal velocity is 2.8–3.1 times that of the particle velocity in the ambient air ($v_{\text{vib}}/v_{\text{air}} = 3.0 \pm 0.3$), whereas this ratio is significantly lower for females, ranging between 1.7 and 2.4 ($v_{\text{vib}}/v_{\text{air}} = 2.1 \pm 0.3$; $P < 0.01$). When the antennal velocities are converted into antennal displacements, with the particle velocity v_{air} being arbitrarily set to 1 mm s^{-1} , the displacement of the flagellar

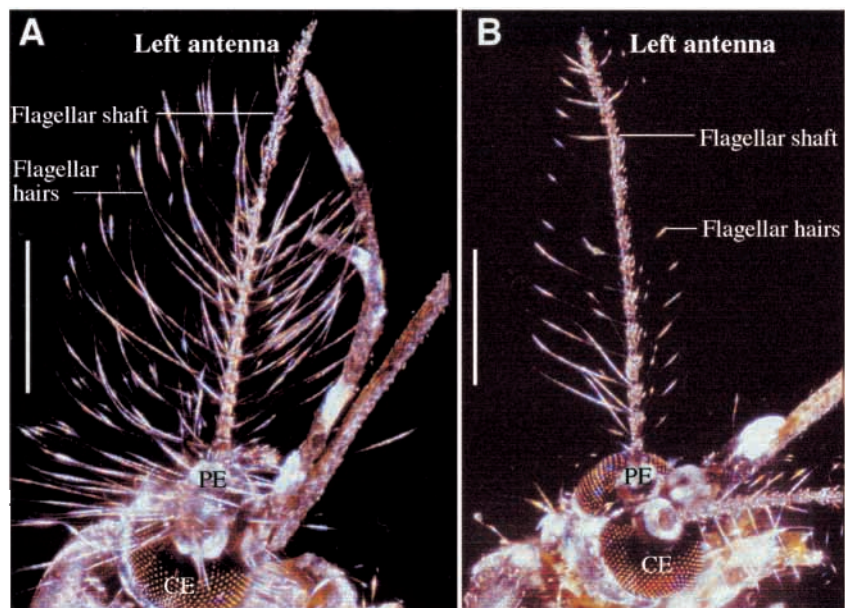
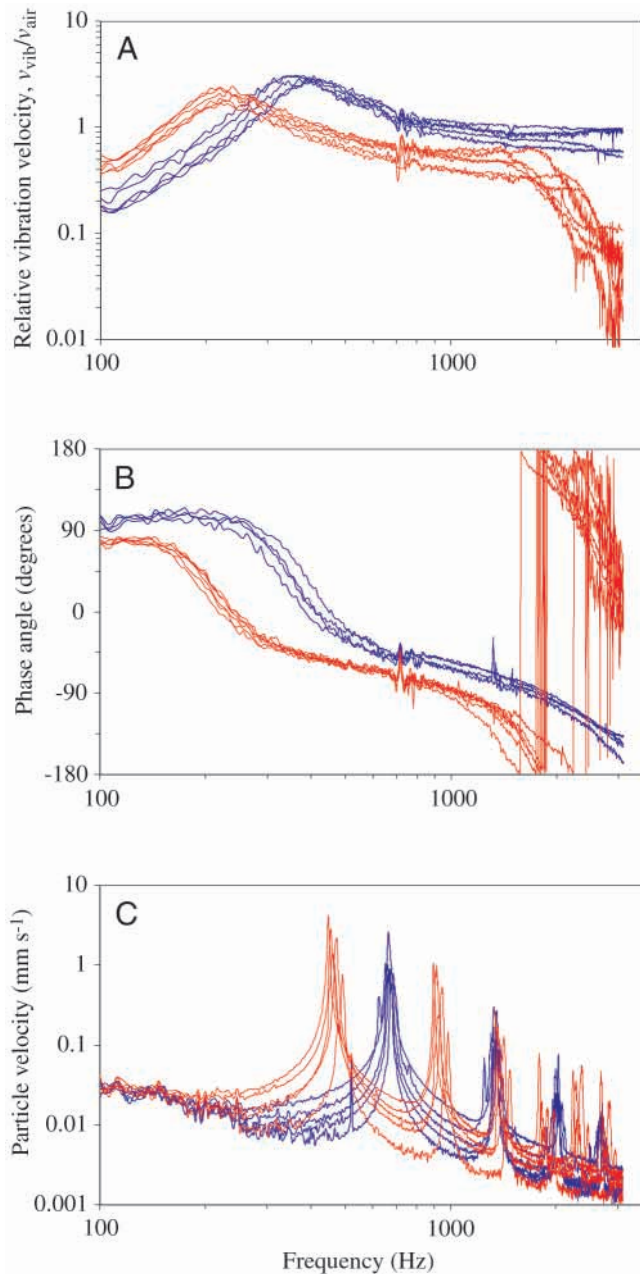


Fig. 5. Light scanning micrographs showing the structure of the antennal flagellum in male (A) and female (B) *Aedes aegypti*. The second antennal segment, the pedicel (PE), contains Johnston's organ, which senses vibrations of the antennal flagellum. Sex-specific differences in the flagellar structure are the number and length of the flagellar hairs and the length of the flagellum, which is shorter in the males than in the females. CE, right compound eye; PE, pedicel of the left antenna. Scale bars, 0.5 mm.



tip of the male antenna at best frequency is approximately $3.0 \times 10^{-3} \text{ m s}^{-1} / 2\pi 380 \text{ s}^{-1} \approx 1.3 \mu\text{m}$ and that of the female antennae is approximately $2.1 \times 10^{-3} \text{ m s}^{-1} / 2\pi 230 \text{ s}^{-1} \approx 1.5 \mu\text{m}$.

A comparison between the frequency characteristics of the antennal vibrations and the frequency composition of the flight sounds (Fig. 6A,C) reveals that the male antenna is tuned approximately to the female flight sounds. The flight sounds of *Aedes aegypti* have a harmonic structure with the fundamental frequency being the dominant component. The fundamental frequency varies between approximately 650 and 680 Hz in males ($668 \pm 10 \text{ Hz}$, $N=6$) and between approximately 445 and 475 Hz in females ($459 \pm 11 \text{ Hz}$, $N=6$; $P < 0.01$). Thus, the best frequency of the male antenna corresponds roughly with the fundamental frequency of female flight sounds with an average

Fig. 6. Frequency response of the antenna measured at the tip of the flagellum and frequency composition of the flight sounds in female (red) and male (blue) *Aedes aegypti*. (A) The magnitude of the antennal vibration velocity v_{vib} relative to the particle velocity v_{air} of the sound field. (B) The phase angle between the phase of the antennal vibration velocity v_{vib} and the phase of the particle velocity v_{air} of the sound field. (C) Frequency spectra of the flight sounds emitted by tethered flying animals. The particle velocity of the sounds was measured at a distance of 10 mm in front of the head of the animals. The figures show superpositions of measurements from different animals (five males and six females for A and B, and five males and five females for C). All measurements of both antennal vibrations and flight sounds were made on the same day from animals belonging to the same generation.

mismatch of approximately 80 Hz. In contrast, the fundamental frequency of the sounds produced by males is quite different from the frequency of best mechanical response (average mismatch approximately 290 Hz), and the tuning of the female antenna does not match the flight sounds of males or of females (average respective mismatch approximately 440 Hz and 230 Hz).

Vibrations of the flagellar shaft and hairs – deflection shapes

To examine whether the vibration response of the flagellar tip reflects that of the whole flagellar shaft, we measured the mechanical response at various positions along the flagellum, with the single measuring spots being distributed equidistantly along the shaft. In total, seven male and seven female antennae were tested, and representative examples are shown in Fig. 7. Comparisons of the vibrations at these different locations show that the resonance peak measured at the flagellar tip can also be traced along the whole shaft. When stimulated at frequencies below or around the best frequency, the magnitude of the relative vibration response of male and female antennae decreases linearly from the tip to the proximal part of the flagellum (Fig. 7A,C). The vibrations at the different measuring points are exactly in phase (Fig. 7B,D). Thus, the flagellum moves like a stiff rod rocking about its socket in response to acoustic stimulation at frequencies corresponding to the first mode of vibration (Fletcher, 1992). Non-linearities become apparent when the flagellum is stimulated at higher frequencies, when the shaft begins to bend. Bending is observed for frequencies above approximately 800 Hz in females and above approximately 2000 Hz in males. This is indicated by the increased phase shift between the vibrations of the distal and proximal regions of the shaft and by the decrease in the relative velocity magnitude, which is smaller at the tip than in the proximal part of the flagellum. These magnitude and phase characteristics indicate that the flagellar shaft enters its second vibration mode. The vibrational response of the proximal, but not of the distal, region of the female flagellum shows a second resonance peak around 1500 Hz, reflecting the frequency of a second mode (Fig. 7C,D). 1500 Hz is approximately 6.4 times the fundamental frequency identified for the first mode (1500 ± 0.3 , mean \pm s.d., $N=7$). This value agrees remarkably

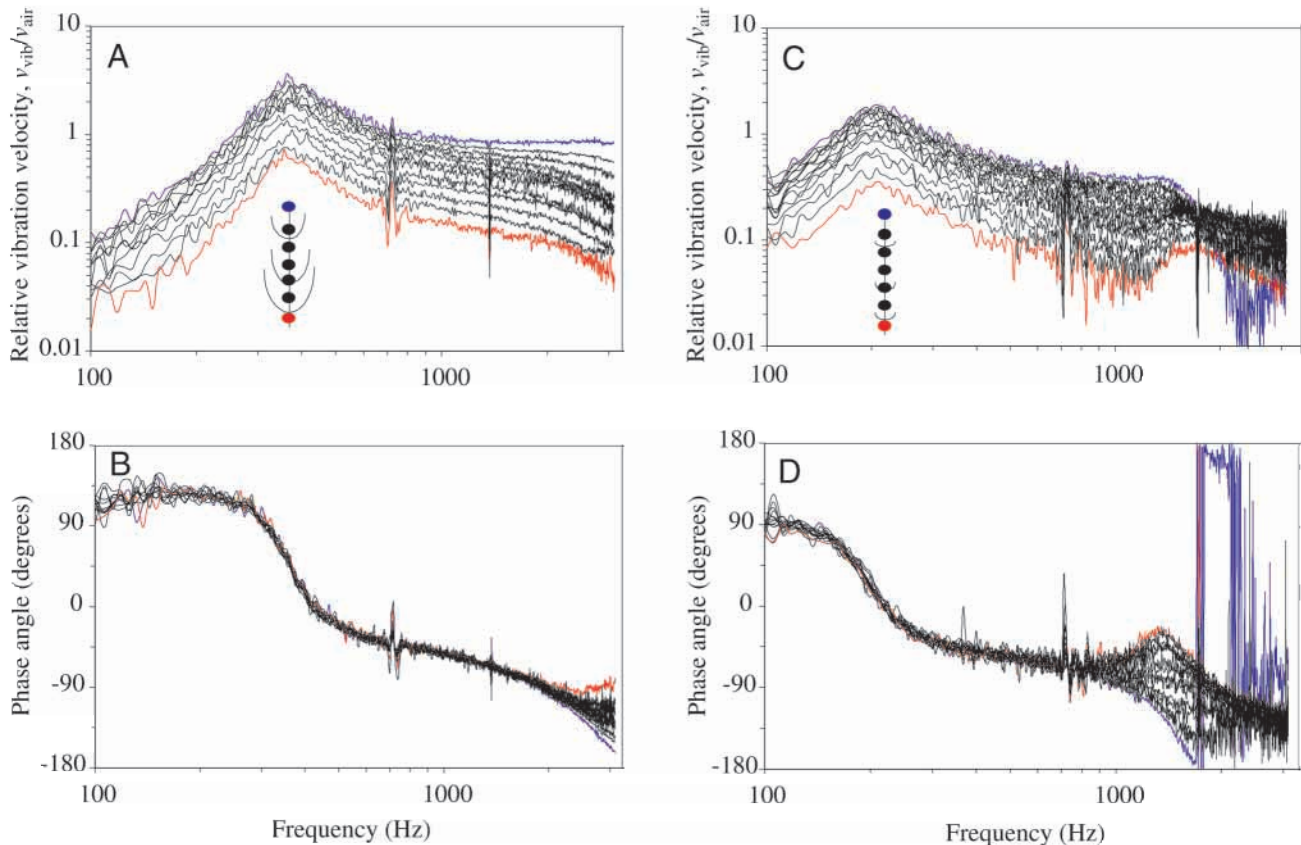


Fig. 7. Frequency responses measured at different heights on the flagellar shaft in a male (A,B) and a female (C,D). The measuring points were distributed equidistantly along the shaft. The response of the antennal tip is shown in blue and that of the base in red. (A,C) The magnitude of the antennal vibration velocity v_{vib} relative to the particle velocity v_{air} of the sound field. (B,D) The phase angle between the phase of the antennal vibration velocity v_{vib} and the phase of the particle velocity v_{air} of the sound field.

well with the factor of 6.3 expected for a freely vibrating rigid bar clamped at one end (Fletcher, 1992). Although the vibration response of the male flagellum should show a comparable second resonance peak at frequencies around 2400 Hz, this was not observed in the range of frequencies tested (Fig. 7A,B). Furthermore, in males, the phase spectrum above 1000 Hz did not reveal any resonance, unlike that of females, for which a phase shift occurs at around 1500 Hz (Fig. 7D). However, the phase characteristics of the male flagellum at frequencies around 3000 Hz are similar to those of the female flagellum at frequencies below the second resonance peak. Thus, the mode frequencies appear to be more separated in the males. This effect is further confirmed by the vibrational response of the shaft demonstrated in Fig. 8, which shows, at approximately 3000 Hz, the lower flank of a second resonance peak.

Analysis of the vibrational behaviour of the antennal hairs (the fibrils) was possible for male antennae only. In contrast to the flagellar shaft of males, the vibrational responses of the antennal hairs show two distinct resonance peaks in the frequency range studied – one at approximately 380 Hz, the same as that of the shaft, and a second one near 2800 Hz (Figs 8, 9). A comparison between the hair-tip vibrations and the shaft vibrations measured at the same height on the same antenna (Fig. 8) shows that the hair and the shaft vibrate with the same

magnitude and phase at frequencies around the lower resonance peak. Only the hair demonstrates a second resonance peak at approximately 2800 Hz. The mechanical response of the hair leads that of the flagellar shaft by approximately 45° and lags the particle velocity in the surrounding air by approximately 45° (Fig. 8). Hence, the lower resonance peak of the hairs reflects vibrations of the whole antenna, whereas the second peak reflects vibrations of the hairs relative to the shaft. Obviously, the hairs of the male antenna have their own resonant tuning. Measurements of the hair-tip vibrations of different hairs inserting at different heights on the same antenna show a similar frequency tuning, with the best frequencies ranging between 2600 and 3100 Hz (Fig. 9). The vibration velocities v_{vib} measured at the hair tips are 0.4–1.6 times that of the particle velocity v_{air} ($v_{\text{vib}}/v_{\text{air}}=0.87\pm 0.37$; number of hairs 30, number of animals 3).

To visualise the vibrations of the antennae, deflection shapes were reconstructed from the relative magnitude and the phase of the vibration velocities measured at various locations on the antenna. A total of seven male and seven female antennae were examined, and representative examples are shown in Fig. 10. The reconstructions confirm that, in both sexes, the antennal flagellum moves like a stiff rod rocking about its socket when stimulated at frequencies below or around the best frequency.

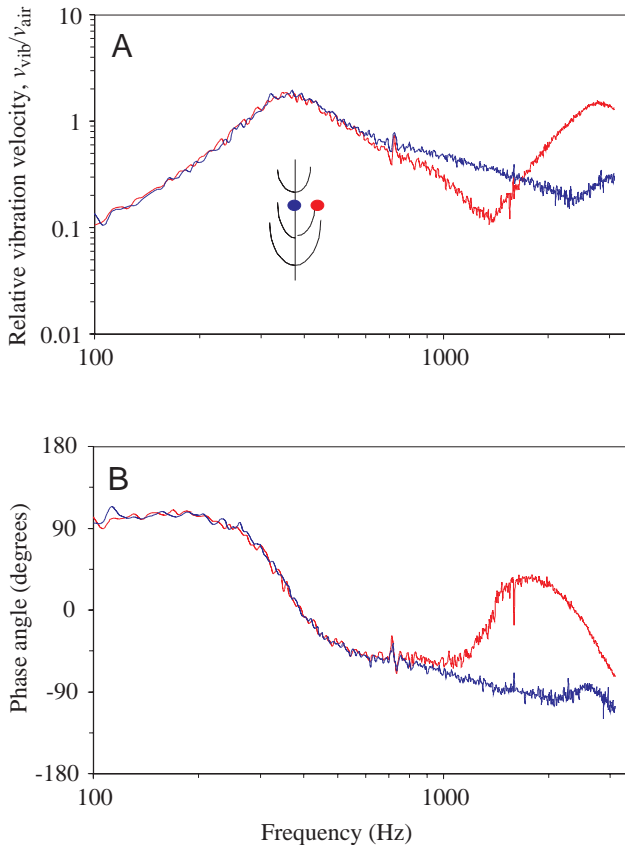


Fig. 8. The frequency response measured at the tip of an antennal hair (red) compared with the frequency response measured at the flagellar shaft (blue) of the same male antenna with both measuring points being located at the same height on the antenna. (A) The magnitude of the antennal vibration velocity v_{vib} relative to the particle velocity v_{air} . (B) The phase angle between the phase of the antennal vibration velocity v_{vib} and the phase of the particle velocity v_{air} .

In particular, the flagellar hairs of the male antenna follow the vibrations of the flagellar shaft. When stimulated at 1500 Hz, the flagellar shaft of the male antenna still moves like a stiff rod, but the flagellar hairs vibrate relative to the shaft. In females, the deflection shape analysis confirms the presence of a second mode of vibration for the flagellum (Fig. 10). At 3000 Hz, the second mode of vibration is present in both male and female antennae, and the hairs of the male antenna vibrate with high velocities relative to the shaft (Fig. 10, lower panels).

Intensity characteristics

The intensity characteristics of the antennal vibrations were examined by measuring the maximum antennal vibration velocity in response to stimulation with different sound intensities. Since maximum vibration velocity occurs at the antennal tip when it is stimulated at the best frequency, we measured the vibration response of the flagellar tip. The frequency of the pure-tone stimulus was adjusted to each individual antenna tested to match its best frequency. The stimulus intensities were varied arbitrarily, and the vibration

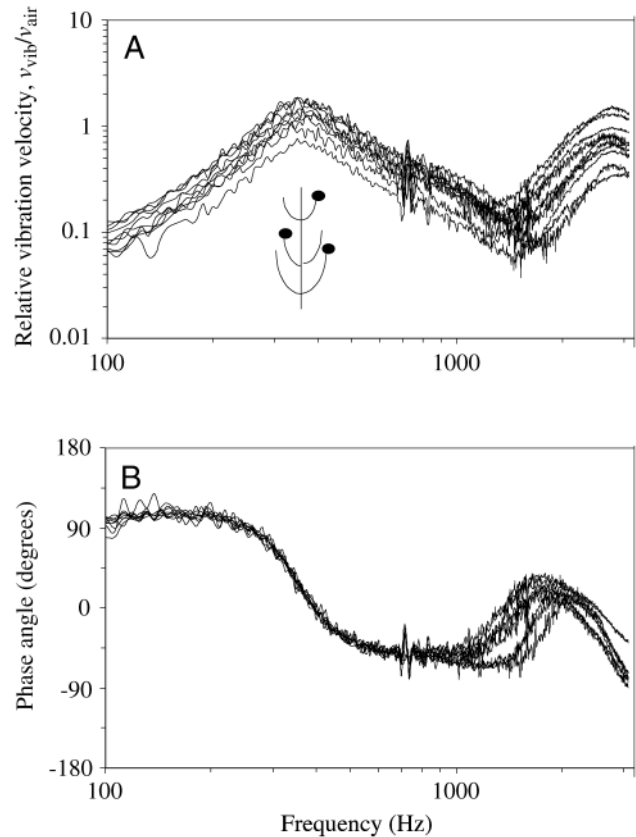


Fig. 9. Frequency responses measured at the tips of different hairs inserting at different heights on the same male antenna. The magnitude (A) and phase (B) of the antennal vibration velocity v_{vib} relative to the particle velocity v_{air} .

velocity of each antenna was measured at 9–15 different intensities corresponding to particle velocities between 0.01 and 30 mm s^{-1} .

In all animals studied (11 males and nine females), the vibration velocity of the antennal tip increased approximately linearly with increasing particle velocity without saturation in the range of particle velocities tested ($P < 0.001$, Spearman rank correlations, one-tailed significance). r^2 values derived for linear regressions of the plots of the antennal velocity v_{vib} against the particle velocity v_{air} vary between 0.97 and 0.99 in the animals studied (Fig. 11A). In accord with the sex-specific differences in relative vibration velocities revealed by the frequency spectra in Fig. 6A, the slopes of the regression lines differ between male and female antennae (Fig. 11A). The slopes of the regression lines, and therefore the ratio of the maximum antennal velocity v_{vib} to the particle velocity v_{air} , vary between 2.2 and 2.7 (2.49 ± 0.19) for males, whereas the slopes calculated for females are significantly lower, ranging from 1.6 to 1.9 (1.78 ± 0.09 ; $P < 0.01$). These values differ slightly from those revealed by the frequency spectra shown in Fig. 6A ($v_{\text{vib}}/v_{\text{air}} \approx 3.0$ for males and $v_{\text{vib}}/v_{\text{air}} \approx 2.1$ for females). The difference can be explained by slight non-linearities in the intensity characteristics of the antennal vibrations. These non-linearities were examined by plotting the ratio of the maximum

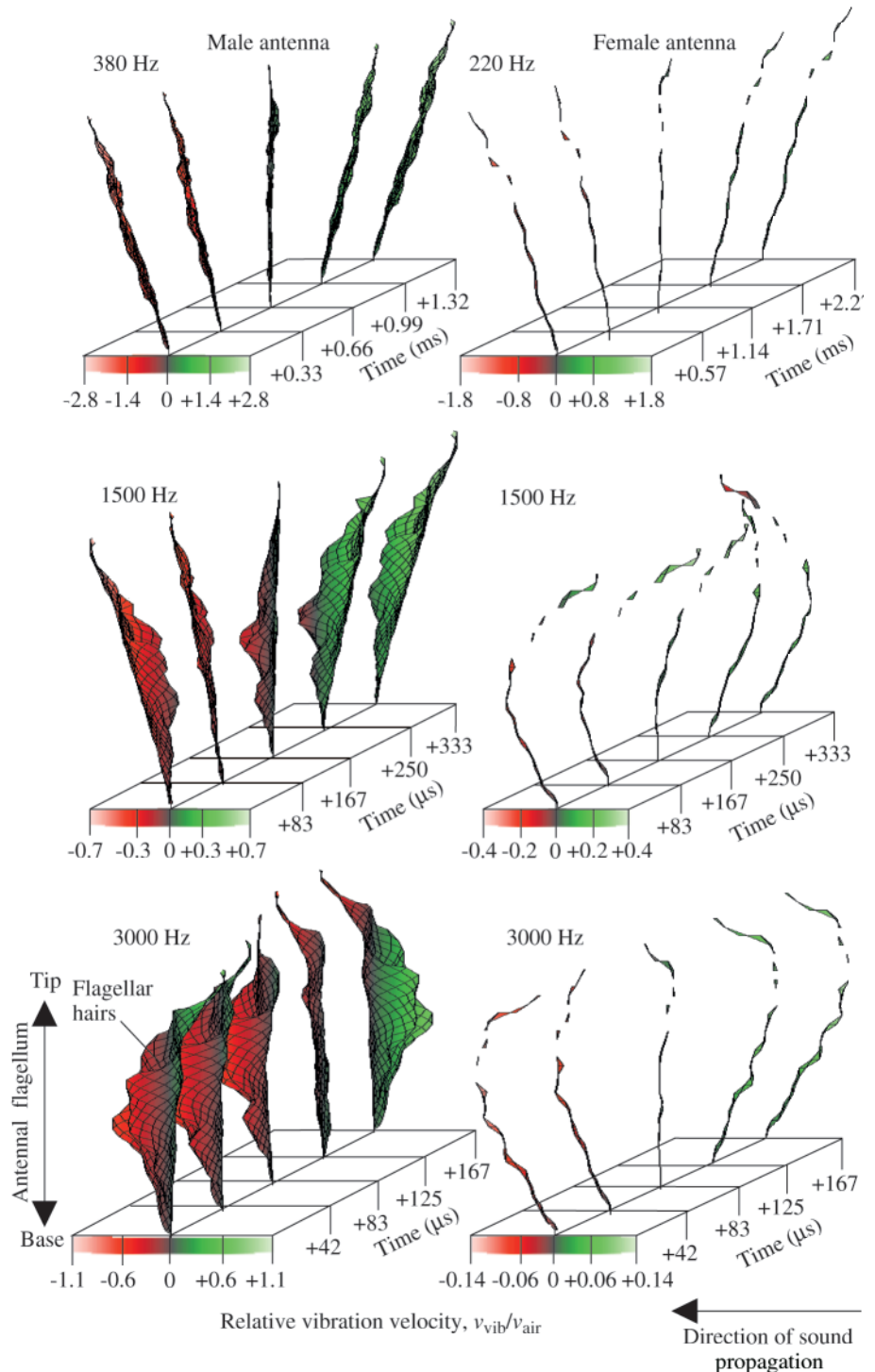


Fig. 10. Deflection shapes of male and female antennae at different frequencies. The deflection shapes were reconstructed from the magnitude and phase of the antennal mechanical response measured systematically at various points on the antennal flagella (laser scanning yielded 267 different measuring points for the male antenna and 37 different valid points for the female antenna). Each of the panels shows the subsequent deflection shapes during half an oscillation cycle. Deflection shapes are viewed from the direction perpendicular to sound propagation.

antennal vibration velocity to the particle velocity $v_{\text{vib}}/v_{\text{air}}$ against the particle velocity v_{air} (Fig. 11B). The velocity ratio $v_{\text{vib}}/v_{\text{air}}$ decreases logarithmically with increasing particle velocity. At a particle velocity of 10 mm s^{-1} , for example, the values of the ratio are approximately 2.6 for the male antenna and approximately 1.8 for the female antenna. At a particle velocity of 0.03 mm s^{-1} , however, the velocity ratio is even higher, reaching 3.7 for males and 2.5 for females. Since the slopes of the logarithmic curves differ only slightly between

males and females, the differences in the velocity of the antennae in the two sexes are almost independent of the particle velocity in the velocity range tested, with the male antennae moving 1.4–1.5 times faster than the female antennae.

Discussion

Since Johnston (1855) predicted that the plumose antennae of male mosquitoes served an auditory function, the sense of

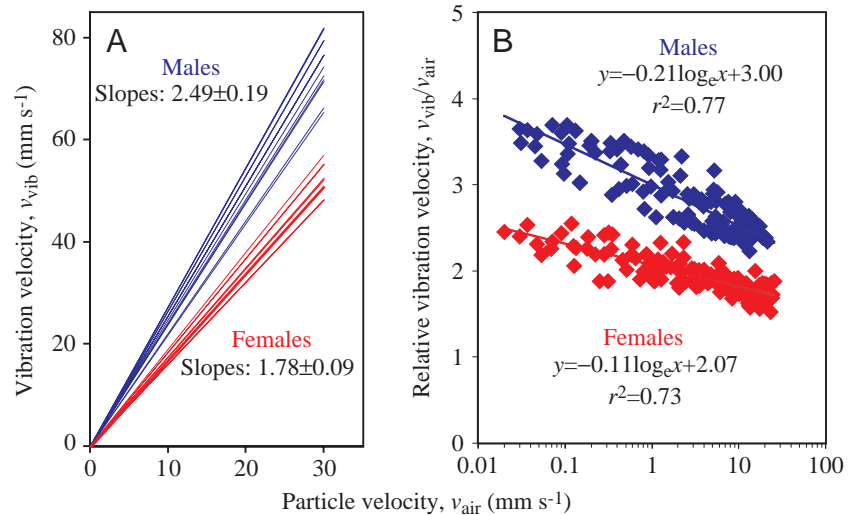


Fig. 11. Intensity characteristics of the antennal vibrations in males and females. (A) Change in the antennal vibration velocity v_{vib} with increasing particle velocity v_{air} . The plot shows linear curve fits to the individual data for 11 males (blue) and nine females (red). The r^2 values of the regressions were greater than 0.97 for all animals studied. (B) Logarithmic curve fits to the plots of the ratio of the antennal velocity to the particle velocity $v_{\text{vib}}/v_{\text{air}}$ against the particle velocity v_{air} (pooled data from 11 males and nine females).

hearing in mosquitoes has attracted the attention of several generations of zoologists (for reviews, see Clements, 1963; Belton, 1974). These studies indicated that male mosquitoes used the flight sounds of conspecific females as acoustic cues for mate detection and correctly attributed an auditory function to Johnston's organ, which is situated in the second antennal segment. The present study provides the first detailed examination of sound-induced antennal vibrations in a mosquito species. The recent development in microscanning laser vibrometry – with its high spatial resolution and high sensitivity – provides a powerful tool for analysing sound-induced vibrations in pressure-sensitive insect ears and other microstructures (Robert and Lewin, 1998). This study demonstrates that the technique is also suited to examine the vibration properties of particle displacement receivers such as mosquito antennae. When stimulated acoustically, the antennae of *Aedes aegypti* move like forced damped harmonic oscillators. At its resonant frequency, the male antenna approximately matches the dominant frequency component of the female flight sounds. Thus, our results strongly support some of the basic assumptions concerning the function of sound perception in mosquitoes and its biological significance. Furthermore, the present examination of the vibration properties of the antennal hairs provides evidence that they are involved in the reception of sound. As pointed out below, the stiff coupling between the hairs and the shaft is a prerequisite for forces acting on the hairs to be transmitted effectively to the shaft and to Johnston's organ.

Antennal mechanics and implications for acoustic attraction

The antennal segments have been reported to serve auditory functions in mosquitoes, drosophilid flies and honeybees. In all three taxa, stroboscopic observations of antennal movements indicated that the antennae move like simple harmonic oscillators with their resonant frequency matching the frequencies of sounds produced by the wing movements of conspecifics (e.g. Tischner and Schieff, 1955; Gould, 1975; Heran, 1959; Bennet-Clark and Ewing, 1967). However, the question of whether the antennae of these insects are indeed

resonantly tuned to specific frequencies remains a matter of debate (e.g. Michelsen and Nocke, 1974; Kirchner, 1994). This problem could not be resolved because accurate identification of resonances requires reliable, coherent information about both the magnitude and the phase characteristics of the antennal mechanical response.

On the basis of coherent magnitude and phase information, the present study confirms that the antennae of *Aedes aegypti* move like simple damped forced harmonic oscillators and constitute resonantly tuned mechanical receivers. Our findings on the difference in tuning between male and female antennae confirm the indications of earlier studies (Tischner and Schieff, 1955). Furthermore, they demonstrate a match between the dominant frequency component of female flight sounds and the male's resonant mechanical response. The difference of 80 Hz between the best frequency of the antenna and female flight sounds may reflect the fact that the flight sounds were recorded from tethered flying animals. Since fixation of the animals is likely to affect their wingbeat frequency, we expect the actual frequency matching to be better than we observed. The relatively broad tuning of the antennal frequency response compared with the sharp tuning of the flight sounds may ensure that males can perceive female flight sounds despite such slight variations. In contrast, the resonant frequency of the female antenna matches the flight sounds of neither males nor females. Hence, there is no immediate and apparent biological reason for females to be able to hear sounds at these frequencies. Behavioural responses to acoustic stimuli have hitherto been reported only for male mosquitoes (e.g. Roth, 1948; Tischner and Schieff, 1955; M. C. Göpfert and D. Robert, personal observation). Since, by definition, hearing implies both the reception of an acoustic stimulus and the performance of acoustically elicited behavioural responses in a biologically relevant context, the auditory function of the antennae in mosquitoes must be assumed, albeit tentatively, to be absent from females.

A further comparison of the vibrational responses between male and female antennae reveals similar magnitude and phase

characteristics, indicating that the antennal flagella have similar mechanical properties. The different frequency tuning appears to be related to the difference in the length of the flagellum. While in our sample the flagellum of the males was 1.6 mm long, the flagellar length in females was 2 mm. For a bar clamped at one end, resonance is inversely related to the squared length of the bar (Fletcher, 1992). Assuming similar mechanical properties for the antennae, the ratio of the resonant frequency of the shorter male flagellum to the resonant frequency of the longer female flagellum would be expected to be $(2\text{ mm})^2/(1.6\text{ mm})^2 \approx 1.6$. The actual measured value of approximately 1.7 (380 Hz/230 Hz) corroborates this simple theoretical prediction. Another sex-specific difference revealed by our study is that the mode frequencies are more widely separated in males than in females, suggesting a significant difference in bending stiffness. The greater stiffness of the male flagellum may minimise the tendency of the shaft to bend at higher stimulus frequencies. Interestingly, the flagellum of male *Aedes aegypti* has been reported to have an elaborate internal endoskeleton previously unknown in insect antennae (Clements, 1963). At the time, Clements speculated on the role of this particular internal anatomy for increasing the stiffness of the flagellum. The ultrastructure of the female flagellum is currently being investigated in our laboratory at the anatomical and biomechanical levels in relation to its stiffness and mechanical response (M. C. Göpfert, H. Cattelan and D. Robert, in preparation).

The possible auditory function of the antennal hairs

According to the existing literature, the sense of audition in mosquitoes appears to be restricted to males (Clements, 1963). Male mosquitoes differ conspicuously from females in that their antennae are plumose, bearing a large number of long hairs. Given this apparent correlation between the structure and function of the mosquito antenna, the long antennal hairs of male mosquitoes have been assumed to be involved in sound perception. The results presented show that the antennal hairs of male *Aedes aegypti* resonate at frequencies around 2600 and 3100 Hz, which is higher than the best frequencies of all arthropod sensory hairs serving as near-field sound receivers that have hitherto been studied (e.g. Tautz, 1979; Kämper and Kleindienst, 1990; Barth et al., 1993; Kumagai et al., 1998). The tuning of the antennal hairs does not match the dominant frequency component of female flight sounds. There is no other apparent biological reason for male mosquitoes to be sensitive to sounds at around 2700–2900 Hz.

The fact that the antennal hairs resonate at higher frequencies only indicates that they are stiffly coupled to the shaft. Experimentally, this is illustrated by the fact that the hairs vibrate relative to the shaft only when stimulated at frequencies above 1000 Hz. When stimulated at biologically relevant frequencies (350–500 Hz), the hairs undergo a displacement that is in phase with that of the shaft, suggesting that the biologically significant mechanical property of the hairs is to provide a stiff coupling between the vibrations of the hairs and those of the shaft. In this way, forces acting on the hairs are

effectively transmitted to the shaft and therefore to Johnston's organ. Thus, stiffly coupled hairs might actually serve an auditory function by increasing the antennal surface and therefore the drag force acting on the antenna, as was proposed by Tautz (1979). A large array of such hairs might improve the acoustic properties of the antenna and, since the air in the spaces between adjacent hairs is likely to be arrested because of viscous forces (Barth et al., 1993), the plumose flagellum of male mosquitoes may act like a paddle.

Mechanical sensitivity of mosquito antennae: sex-specific differences and comparisons with other arthropod movement receivers

In studies of arthropod sensory hairs serving as movement receivers sensitive to airborne sounds, the ratio of the vibration velocity of the hair tip at its best frequency to the particle velocity in the surrounding air $v_{\text{vib}}/v_{\text{air}}$ (or the equivalent ratio of the hair-tip displacement to the particle displacement) has been used to characterise mechanical sensitivity. Tautz (1977) provided an intuitive model that predicted a theoretical upper limit for the values of this ratio. According to his model, the velocity of a hair tip cannot exceed the particle velocity by more than a factor of 2. This limitation was later confirmed by calculations based on fluid-dynamic considerations (Fletcher, 1978; Humphrey et al., 1993), but it was also noted that the ratio $v_{\text{vib}}/v_{\text{air}}$ depended largely on the geometry of the vibrating system and that higher ratios are at least theoretically possible. The experimental determination of the ratio for different types of insect sensory hairs and spider trichobothria revealed that these movement receivers are characterised by ratios usually smaller than 2, ranging between approximately 0.2 and 2 (e.g. Tautz, 1977; Kämper and Kleindienst, 1990; Barth et al., 1993). The ratio for the antennal hairs of male *Aedes aegypti* lay between 0.2 and 1.6. The velocity ratio reported here for the female antenna also corroborates previous findings (although values above 2 were found at low particle velocities). However, the present biomechanical analysis of the male antenna yields values between 2.6 and 3.7, which constitute the highest values reported so far. The mechanical sensitivity of the male antenna not only exceeds that of conspecific females but also those of all other known arthropod movement receivers.

The velocity ratio decreases logarithmically with increasing particle velocity, and this non-linearity may reflect the increasing stiffness of the flagellar articulation at large deflection amplitudes (see Fletcher, 1992). Nevertheless, the difference between the velocity ratio of male and female antennae is not related to the absolute particle velocity in the range of velocities examined. At a given particle velocity, the male antenna moves 1.4–1.5 times faster than the female antenna. To evaluate the significance of this difference, this ratio must be transformed to angular deflections because the auditory sensory cells in Johnston's organ are probably sensitive to the angular deflection of the flagellum rather than to its vibration velocity. The angular deflection is inversely correlated with frequency and, since the antennae of males are tuned to approximately 380 Hz and those of females to

approximately 230 Hz, the angular deflection of the male antenna at best frequency would be expected to be only 230 Hz/380 Hz, approximately 0.6, times that of the female antenna at its best frequency in the case of identical mechanical sensitivity and antennal length. However, because of sex-specific differences in mechanical sensitivity, the actual angular deflection of the male antenna (at equal particle velocity) is not 0.6 but 0.9 times that of the female antenna. In addition, the shorter male flagellum also gives rise to a larger angular deflection that is not 0.9 times but $0.9/(1.6\text{ mm}/2\text{ mm})$ times, which is approximately 1.1 times that of the female antenna. Thus, the higher mechanical sensitivity and the shorter flagellum of male *Aedes aegypti* together approximately compensate for the angular deflection, which would be expected to be lower in the males than in the females as a result of different frequency tuning.

Many thanks to M. Bergmann and R. Miles for critical reading of the manuscript and to Daniel Huber for light scanning microphotography. The authors were supported by research grants from the Swiss National Science Foundation (D.R., H.B.) and a fellowship from the Deutscher Akademischer Austauschdienst (DAAD) (M.C.G.).

References

- Barth, F. G., Wastl, U., Humphrey, J. A. C. and Devarakonda, R.** (1993). Dynamics of arthropod filiform hairs. II. Mechanical properties of spider trichobothria (*Cupiennius salei* Keys.). *Phil. Trans. R. Soc. Lond. B* **340**, 445–461.
- Belton, P.** (1974). An analysis of direction finding in male mosquitoes. In *Experimental Analysis of Insect Behaviour* (ed. L. B. Browne), pp. 139–148. Heidelberg, New York: Springer.
- Bennet-Clark, H. C.** (1971). Acoustics of insect song. *Nature* **234**, 255–259.
- Bennet-Clark, H. C.** (1984). A particle velocity microphone for the song of small insects and other acoustic measurements. *J. Exp. Biol.* **108**, 459–463.
- Bennet-Clark, H. C.** (1999). Which Qs to choose: Questions of quality in bioacoustics. *Bioacoustics* **9**, 351–359.
- Bennet-Clark, H. C. and Ewing, A. W.** (1967). Stimuli provided by the courtship of male *Drosophila melanogaster*. *Nature* **215**, 669–671.
- Clements, A. N.** (1963). *The Physiology of Mosquitoes*. Oxford, London, New York, Paris: Pergamon Press.
- Fletcher, N. H.** (1978). Acoustical response of hair receptors in insects. *J. Comp. Physiol. A* **127**, 185–189.
- Fletcher, N. H.** (1992). *Acoustic Systems in Biology*. New York, Oxford: Oxford University Press.
- Gould, J. L.** (1975). Honey bee communication: the dance-language controversy. Thesis, Rockefeller University, New York.
- Heran, H.** (1959). Wahrnehmung und Regelung der Flugeigengeschwindigkeit bei *Apis mellifera* L. *Z. Vergl. Physiol.* **42**, 103–163.
- Hoy, R. R. and Robert, D.** (1996). Tympanal hearing in insects. *Annu. Rev. Ent.* **41**, 433–450.
- Humphrey, J. A. C., Devarakonda, R., Iglesias, I. and Barth, F. G.** (1993). Dynamics of arthropod filiform hairs. I. Mathematical modelling of the hair and air motions. *Phil. Trans. R. Soc. Lond. B* **340**, 423–444.
- Johnston, C.** (1855). Auditory apparatus of the *Culex* mosquito. *Q. J. Microsc. Sci.* **3**, 97–102.
- Kämper, G. and Kleindienst, H.-U.** (1990). Oscillation of cricket sensory hairs in a low-frequency sound field. *J. Comp. Physiol. A* **167**, 193–200.
- Kates, J. M.** (1992). On using coherence to measure distortion in hearing aids. *J. Acoust. Soc. Am.* **91**, 2236–2244.
- Kirchner, W. H.** (1994). Hearing in honeybees: the mechanical response of the bee's antenna to near field sound. *J. Comp. Physiol. A* **175**, 261–265.
- Kumagai, T., Shimozawa, T. and Baba, Y.** (1998). Mobilities of the cercal wind-receptor of the cricket, *Gryllus bimaculatus*. *J. Comp. Physiol. A* **183**, 7–21.
- Mayer, A. M.** (1874). Experiments on the supposed auditory apparatus of the mosquito. *Am. Nat.* **8**, 577–592.
- Michelsen, A. and Nocke, H.** (1974). Biophysical aspects of sound communication in insects. *Adv. Insect Physiol.* **10**, 247–296.
- Nijhout, H. F. and Sheffield, H. G.** (1979). Antennal hair erection in male mosquitoes: a new mechanical effector in insects. *Science* **206**, 595–596.
- Robert, D. and Lewin, A.** (1998). Microscanning laser vibrometry applied to the biomechanical study of small auditory systems. In *Third International Conference on Vibration Measurements by Laser Techniques, Ancona, Italy* (ed. E. P. Tomasini), pp. 564–571. *Proceedings of the International Society of Optical Engineering, Washington, USA*.
- Roth, L. M.** (1948). A study of mosquito behaviour. An experimental laboratory study of the sexual behavior of *Aedes aegypti* (Linnaeus). *Am. Midl. Nat.* **40**, 265–352.
- Shimozawa, T., Kumagai, T. and Baba, Y.** (1998). Structural scaling and functional design of the cercal wind-receptor hairs of cricket. *J. Comp. Physiol. A* **183**, 171–186.
- Tautz, J.** (1977). Reception of medium vibration by thoracic hairs of caterpillars of *Barathra brassicae* L. (Lepidoptera, Noctuidae). *J. Comp. Physiol. A* **125**, 67–77.
- Tautz, J.** (1979). Reception of particle oscillation in a medium – an unorthodox sensory capacity. *Naturwissenschaften* **66**, 452–461.
- Timmermann, S. E. and Briegel, H.** (1993). Water depth and larval density affect development and accumulation of reserves in laboratory populations of mosquitoes. *Bull. Soc. Vector Ecol.* **18**, 174–187.
- Tischner, H. and Schieff, A.** (1955). Fluggeräusch und Schallwahrnehmung bei *Aedes aegypti* L. (Culicidae). *Zool. Anz.* **18** (Suppl.), 453–460.
- Wishart, G. and Riordan, D. F.** (1959). Flight responses to various sounds by adult males of *Aedes aegypti* (L.) (Diptera: Culicidae). *Can. Ent.* **91**, 181–191.
- Wishart, G., van Sickle, G. R. and Riordan, D. F.** (1962). Orientation of the males of *Aedes aegypti* (L.) (Diptera: Culicidae) to sound. *Can. Ent.* **94**, 613–626.